doi:10.3969/j.issn.1673-9736.2017.04.03
Article ID: 1673-9736(2017)04-0208-09

Geochronology and geochemistry of Hutouya monzonitic granite of Qimantage, Qinghai

WANG Yang[1], SUN Fengyue[1], GAO Hongchang[1], HE Shuyue[2], QIAN Ye[1] and XU Chenghan[1]

1. *College of Earth Sciences, Jilin University, Changchun 130061, China;*
2. *The Third Institute of Qinghai Geological Mineral Prospecting, Xining 810029, China*

Abstract: The geochemical features of the monzonitic granite in Qimantage Hutouya deposit area, Qinghai, in respect to the mineralization, suggest that this granite belongs to weak peraluminous and high-k calc alkaline rock series. The REE of the samples show right slope with obvious LREE/HREE differentiation and negative Eu abnormity. The trace elements show enrichment of LILE (Rb, Th, U, La, Nd), and deleption of Ba, Sr, Nd, P, Ti. The Sr-Nb isotopic data indicate that the magma source is mainly aluminosilicate lower crust with a small amount of new crustal materials. The weighted mean zircon U-Pbage of the Hutouya monzonitic granite is 221 ± 1.7 Ma, belonging to Late Triassic. The Hutouya monzonitic granite was formed in the tectonic setting of transition from compression to extension during Middle-Late Triassic.

Key words: monzonitic granite; zircon U-Pb age; geochemistry; Hutouya; Qimantage; Qinghai

0 Introduction

Hutouya of Qimantage, Qinghai is located in the northern slope of the Qimantage Mountain of the eastern Kunlun, and the north of the Kunbei fault and the Nalingguolehe fault. Tectonically, it is located in the western section of East Kunlun orogenic belt, Qinghai, surrounded by the Qaidam block, East Kunlun orogenic belt and the Alytn fault belt. In Qimantage, there exist a lot of porphyry-type and skarn type deposits related to intermediate acid intrusive body of Indo-Chinese epoch. The Indo Chinese epoch is an important metallogenic epoch with widespread magmatism. The Hutouyapoly metallic deposit in Qimantage of Qinghai is a typical skarn-type deposit with certain scale in the Qimantage metallogenic belt, and the characteristics and metallogenic regularity of ore deposits have universality.

The previous studies are mostly related to the geological characteristics, genesis of ore deposit, source of material and geophysical characteristics (Feng *et al.*, 2011; Zhang *et al.*, 2013; Gao *et al.*, 2013; Zhang *et al.*, 2012). But not much on zircon U-Pb geochronology and geochemical characteristics of ore-forming rocks, therefore, this study chose the monzonitic granite of Hutouya deposit area as research object related to polymetallic mineralization, and carried out the studies of geochronology and geochemistry of rocks, in order to understand the genesis of rock and its tectonic setting, identify of the diagenetic age, provide the evidences for the metallogenic epoch and magmatism in the area.

Received 20 December 2016, accepted 25 January 2017
Supported by Project of China Geological Survey (No. 20150209-01-079)

1 Geological background

Hutouya deposit area is located in the downstream of the Wuyi river, and the west of the Qimantage magmatic arc belt, where developed a lot of multiple intermediate acid intrusive rocks and old basement rock series with high degree of consolidation (Langyashan Fm.) and Tanjianshan Group. The strata include Middle Proterozoic Langyashan Formation, Ordovician-Silurian Tanjianshan Group, Lower Carboniferous Dagangou Formation, Upper Carboniferous Di'aosu Formation, the Upper Triassic E'lashan Formation and Quaternary (Fig. 1). The intrusive rocks are mainly Late Triassic porphyraceous monzonitic granite, granodiorite, moyite and diorite. The granodiorite and monzonitic granite has relationship with the mineralization (Zhang *et al.*, 2013; Feng *et al.*, 2011). The fault structure is dominant, which are mainly the near EW-trending fault sets and secondly NE-trending fault sets. The near EW-trending compression torsion fault is the main structural framework in the area, controlling the sedimentary formation, magmatism, metamorphism and mineral formation. There are nine ore belts and 117 metal ore bodies of Cu, Fe, Pb, Zn and Ag in the deposit area. Multi metal resources (Cu-Pb-Zn and so on) of the whole area are estimated at about a million tons. The omulti-metal deposits can be up to large scale and the Fe-Sn deposits is in small scale.

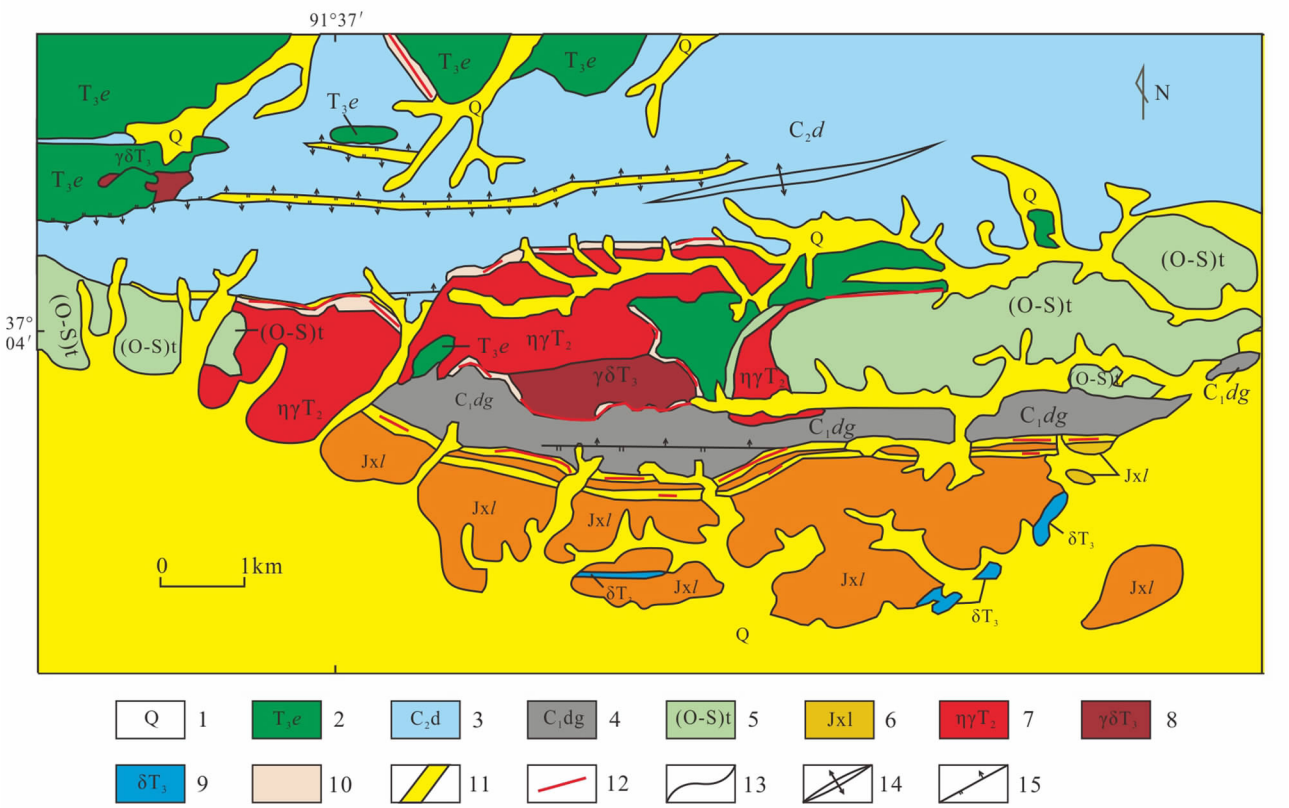

1. Quaternary; 2. Upper Triassic E'lashan Fm. (crystal tuff, rhyolitic brecciated tuff andrhyolitic vitric tuff breccia clasts); 3. Upper Carboniferous Diaosu Fm. (microcrystalline limestone, microcrystalline-fine crystalline dolomite, dolomitic limestone, marble, bio-clastic limestone, feldspar quartz sandstone andhornfels); 4. Lower Carboniferous Dagangou Fm. (marble interlayered with limestone); 5. Ordovician-Silurian Tanjianshan basalt and tuff interlayered with silicalite; 6. Jixianian System Langyashan Fm. (calcite dolomite, carbonaceous mud crystalline limestone, marble, quartz sandstone, sericite slate and siliceous rocks; 7. Late Triassic monzonitic granite; 8. Late Triassic granodiorite; 9. Late Triassic diorite; 10. skarn; 11. fractured alteration zone; 12. ore body; 13. geological boundary; 14. anticline; 15. reverse fault.

Fig. 1 Geological map of Qimantage-Hutouya of Qinghai (after Zhang *et al.*, 2013)

2 Petrographic characteristics

The monzonitic granite in the deposit area is chosen as the research object (Fig. 2). The rock is light red, medium to fine grained, composed of potassium feldspar (35%–40%), plagioclase (30%–45%), quartz (20%–30%), biotite (3%–5%) and minor apatite, zircon, tourmaline. The potassium feldspar is hypautomorphic plate and perthite with poikilitic of quartz and plagioclase, forming graphic texture with quartz, with slight kaolinization. The plagioclase is euhedral plate with polysynthetic twin, and mainly consists of oligoclase with sericitization, epidotization and carbonization. The quartz is hypautomorphic granular with eroded margin and partly epigenetic or exotic, and has carbonization and muscovitization.

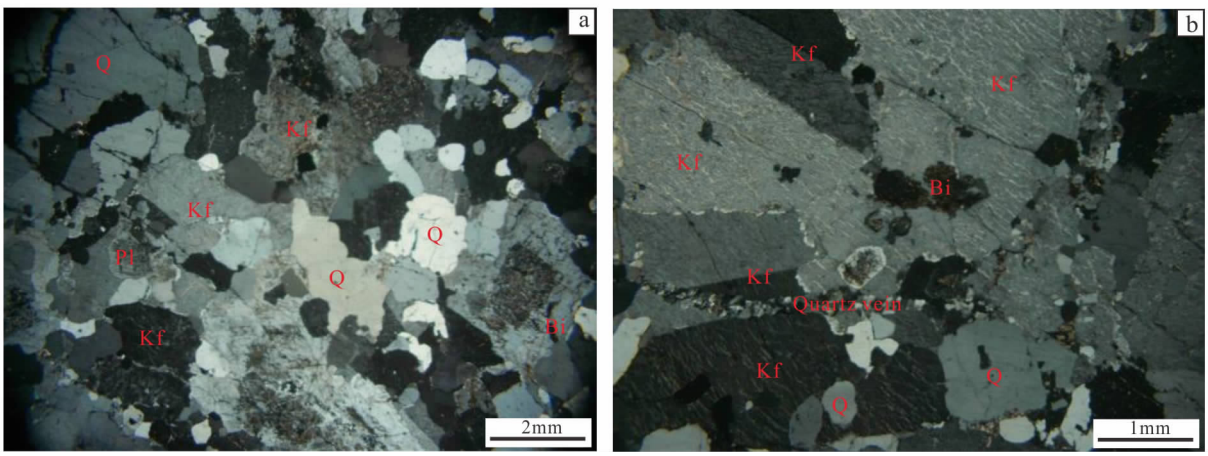

(a) HTY-20-1 xenomorphic-hypautomorphic grain structure of monzonitic granite (+); (b) HTY-20-2 perthite of monzonitic granite (+). Kf: potash feldspar Q: quartz Pl: plagioclase Bi: biotite.

Fig. 2 Microscope images of Hutouyamonzonitic granite

3 Analysis method

Zircons were selected in the Regional Geological Survey Institute of Langfang, Hebei. The zircons with different length-width ratio, cone features and colors are chosen by the binocular microscope. Crystal morphology and internal texture of zircon were studied by the reflected light and CL image, and the best analysis points were selected. The target, reflected light, cathode luminescence image acquisition and dating analysis of zircon were completed by the State Key Laboratory of continental dynamics of Northwestern University. The specific analysis methods and procedures can be seen in Yuan *et al.* (2003, 2004), Anderson (2002), Liu *et al.* (2008) and Liu *et al.* (2010). Age calculation and drawing were completed by the Isoplot (Ludwig, 2003).

The major and trace element analysis was completed in the Analysis Centre of Beijing Geological Research Institute. The major elements are analyzed by the X-ray fluorescence spectrometer (Philips PW 2404), and the detection limit of Al_2O_3, Si_2O, MgO, Na_2O is 0.015%, while the detection limit of CaO, K_2O, TiO_2 is 0.01% and the detection limit of Fe_2O_3T, MnO, P_2O_5 is 0.005%. The analysis of Fe is carried out by volumetric method (the detection limit = 0.1%). The analysis of trace elements was carried out by inductively coupled plasma mass spectrometry, Fining MAT-ICP-MS (Element Ⅰ-type), and the specific analysis methods and procedures have been described by Qi (2000).

In situ micro region zircon Hf isotopic analysis was completed in the State Key Laboratory of Geological Processes and Mineral Resources (GPMR) of China University of Geosciences (Wuhan). The analysis was carried out by laser ablation multiple receiving plasma (LA-MC-ICP-MS). Laser ablation system

is GeoLas 2005 (Lambda Physik, German). The MC-ICP-MS is Neptune Plus (Thermo Fisher Scientific, German). Single point erosion model is used, and the spot beam is 44 μm. Specific operating conditions and analytical methods have been described in Hu *et al.* (2012), Fisher *et al.* (2014) and Blichert-Toft *et al.* (1997). Offline processing of analytical data is carried out by ICP-MS Data Cal (Liu *et al.*, 2010).

4 Analysis result

4.1 Zircon U-Pb chronology

Zircons in sample 1217I (monzonitic granite) are idiomorphic with well-developed surface plane, and the long column is dominant with crystal axis ratio 1∶1 to 2∶1 and minor short column. Cathodoluminescence image (CL) shows clear oscillatory zoning, indicating a magmatic origin (Fig. 3). The results of 18 analysis points (Table 1) show that the U content is

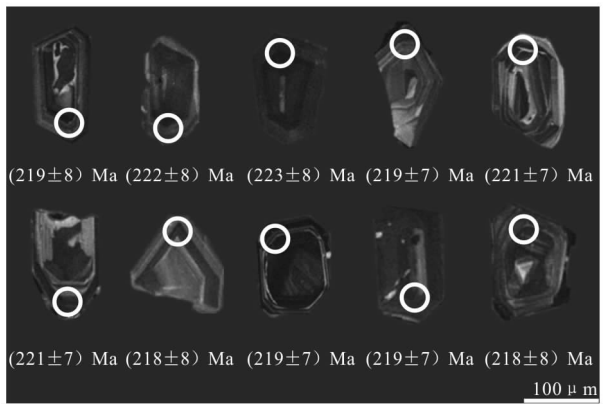

Fig. 3 Cathodoluminescence (CL) images from samples from granite in Hutouya

Table 1 Zircon U-Pb isotopic dating of monzonitic granite in Hutouya

Samples	$^{238}U/10^{-6}$	$^{232}Th/10^{-6}$	Th/U	$^{207}Pb/^{206}Pb$		$^{207}Pb/^{235}U$		$^{206}Pb/^{238}U$		$^{206}Pb/^{238}U$	
				Ratio	1σ	Ratio	1σ	Ratio	1σ	Age/Ma	1σ
1217I007	251.07	116.98	0.465925837	0.05194	0.00409	0.24705	0.01924	0.0345	0.00125	219	8
1217I008	621.6	111.27	0.179005792	0.05097	0.00372	0.24603	0.01776	0.03501	0.00125	222	8
1217I010	344.18	199.6	0.579929107	0.05079	0.00332	0.24605	0.01601	0.03513	0.00121	223	8
1217I012	3710.98	854.97	0.230389277	0.05224	0.00186	0.24863	0.00908	0.0345	0.00112	219	7
1217I013	662.29	184.6	0.278729862	0.05109	0.00301	0.24636	0.01446	0.03495	0.00118	221	7
1217I018	3501.07	665.06	0.18995907	0.05037	0.00178	0.24218	0.00879	0.03484	0.00112	221	7
1217I019	361.36	132.34	0.366227585	0.05165	0.00471	0.24482	0.02204	0.03435	0.00126	218	8
1217I020	272.81	133.34	0.488765075	0.0506	0.00352	0.24123	0.01662	0.03454	0.00119	219	7
1217I021	393.21	174.54	0.443884947	0.05067	0.00322	0.24147	0.01524	0.03453	0.00117	219	7
1217I024	254.39	136.23	0.535516333	0.05068	0.00647	0.24064	0.03031	0.0344	0.00135	218	8
1217I025	480.13	184.9	0.385104034	0.05107	0.00281	0.24568	0.01352	0.03486	0.00114	221	7
1217I026	494.25	176.85	0.357814871	0.05097	0.00349	0.24662	0.01675	0.03506	0.00118	222	7
1217I027	2139.87	752.41	0.351614818	0.05685	0.00202	0.28094	0.01018	0.03581	0.00113	225	7
1217I028	447.78	249.36	0.556880611	0.05243	0.0042	0.25604	0.02022	0.03539	0.00125	224	8
1217I032	383.52	117.97	0.307598039	0.05066	0.00372	0.24535	0.01783	0.03511	0.00119	222	7
1217I033	793.08	246.74	0.311116155	0.0505	0.00236	0.24013	0.01122	0.03448	0.0011	219	7
1217I039	538.61	208.25	0.386643397	0.05124	0.00309	0.24803	0.01484	0.03514	0.00115	223	7
1217I042	626.43	173.67	0.27723768	0.05071	0.00404	0.24616	0.01931	0.03526	0.00121	223	8

(251–3 710) $\times 10^{-6}$, the Th content is (111–854) $\times 10^{-6}$, with Th/U ratios of 0.17–0.57. The 18 zircons are in or near the Concordia curve, and the concordia age of the $^{207}Pb/^{235}U$ and $^{206}Pb/^{238}U$ zircon is 221.0 ± 1.7 Ma (MSDW = 0.56) (Fig. 4a). The weighted mean zircon $^{207}Pb/^{206}Pb$ age is 221.0 ± 3.4 Ma

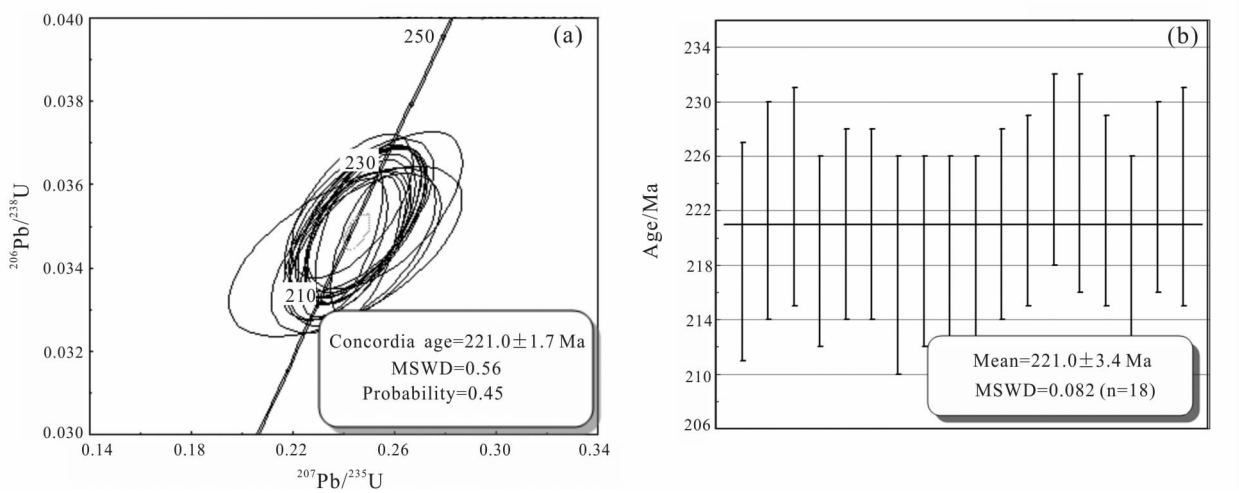

Fig. 4 Concordia diagram (a) and weighted mean ages (b) of zircon U-Pb dating for monzogranite in Hutouya

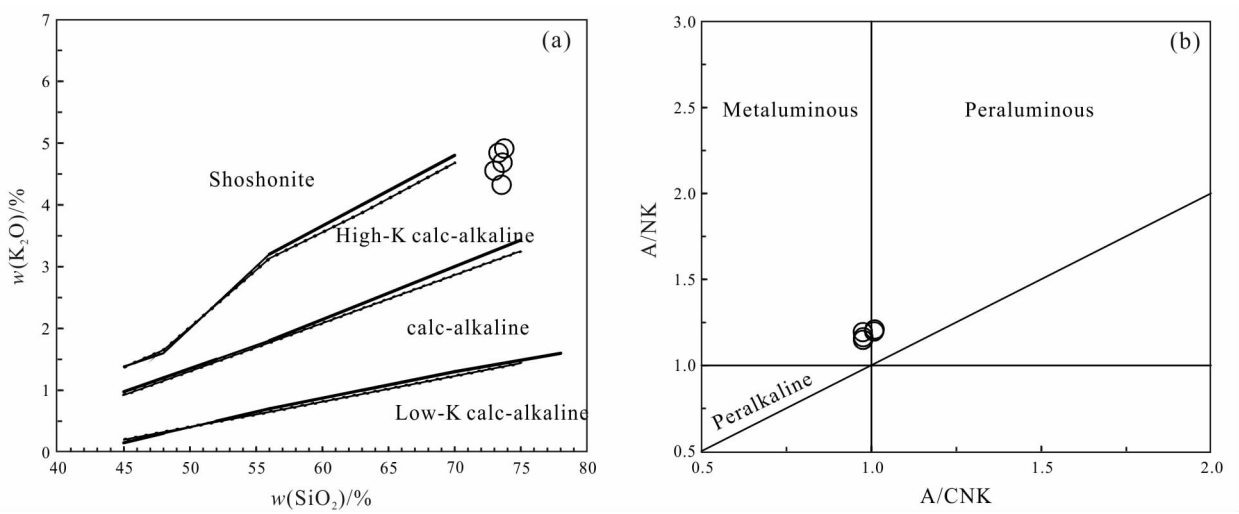

Fig. 5 SiO_2-K_2O diagram (a) and A/CNK-A/NK diagram (b) of Hutouya granite

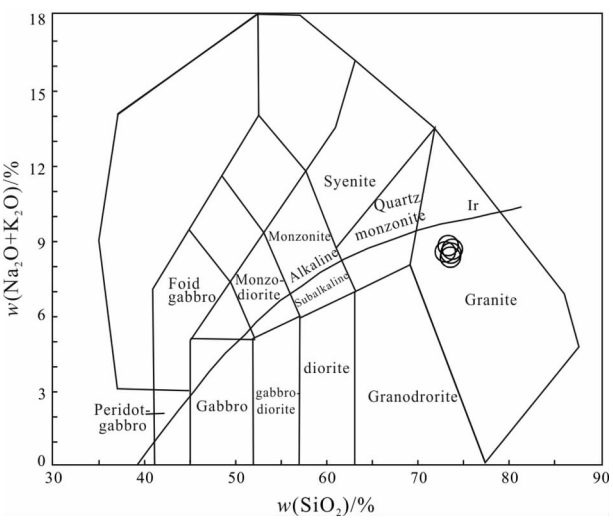

Fig. 6 TAS diagram of Hutouya granite

(MSWD = 0.082) (Fig. 4b), which is similar to the concordia age and can represent the diagenetic age.

4.2 Geochemical characteristics of rocks

4.2.1 Major elements

As shown in the results of the major elements (Table 2), the SiO_2 of the Hutouya monzonitic granite is 73.02%–73.77%. In the Si-alkalinity diagram, the samples plot into the granite field (Fig. 5a). The (K_2O + Na_2O) is 8.21%–8.68%. The K_2O is 7.45%–8.23%. In the $w(K_2O)$–$w(SiO_2)$ (Fig. 5b) and A/NK-A/CNK (Fig. 6), the samples plot into the high-k calc alkaline series and quasi-aluminous field.

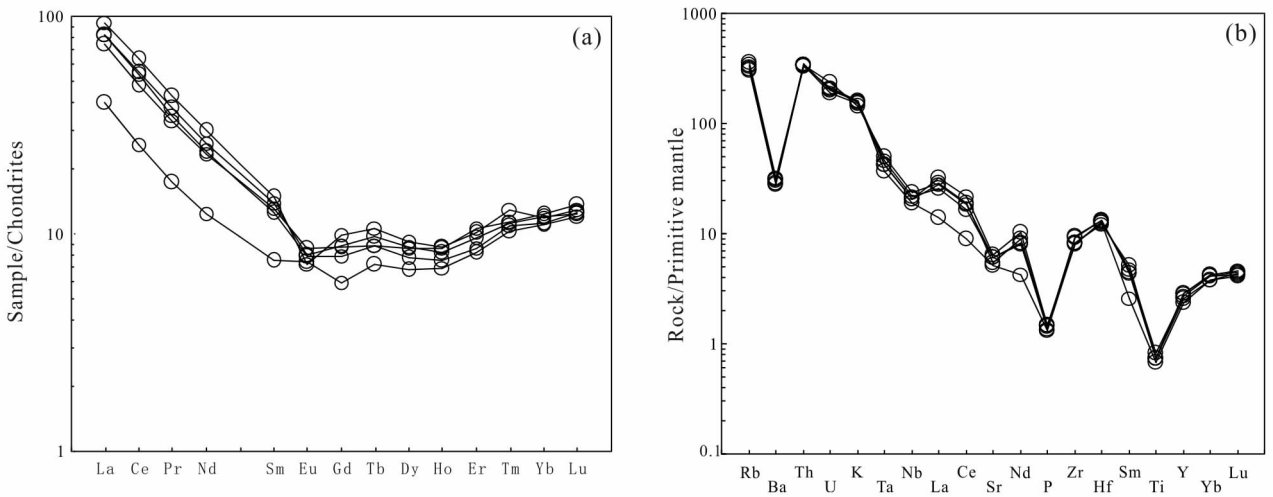

Fig. 7 Chondrite-normalized REE distribution pattern (a) and primitive mantle-normalized trace element spider diagram (b) of Hutouya granite

Table 2 Major (%), REE and trace element content (10^{-6}) and parameter of the granite rocks in Hutouya

Sample	JR-2	JR-3	JR-4	JR-5	JR-6	Sample	JR-2	JR-3	JR-4	JR-5	JR-6
SiO_2	73.63	73.77	73.02	73.32	73.57	Zr	104.00	93.00	93.00	105.00	90.00
TiO_2	0.16	0.15	0.16	0.16	0.18	Th	28.90	28.10	28.60	30.00	28.70
Al_2O_3	13.34	13.09	13.59	13.34	13.20	U	4.40	4.50	4.00	4.20	5.00
Fe_2O_3	2.09	2.18	2.17	2.06	2.14	La	17.70	9.50	22.20	19.40	19.60
MnO	0.10	0.14	0.10	0.09	0.09	Nd	10.90	5.80	14.00	11.20	12.20
MgO	0.27	0.24	0.33	0.27	0.29	Hf	4.10	3.90	3.80	4.10	4.00
CaO	1.07	1.10	1.12	1.09	1.28	Sm	2.01	1.16	2.27	1.92	2.13
Na_2O	3.70	3.62	3.87	3.84	3.89	Eu	0.50	0.43	0.42	0.46	0.46
K_2O	4.68	4.91	4.55	4.84	4.32	Gd	1.78	1.23	2.04	1.63	1.82
P_2O_5	0.03	0.03	0.03	0.03	0.03	Tb	0.33	0.27	0.40	0.33	0.36
LOI	0.53	0.36	0.63	0.58	0.63	Dy	2.19	1.74	2.35	1.98	2.22
Total	99.61	99.58	99.57	99.62	99.62	Ho	0.48	0.40	0.49	0.43	0.47
$Mg^{\#}$	15.48	13.54	17.77	15.67	16.31	Er	1.76	1.30	1.68	1.43	1.58
A/CNK	1.01	0.98	1.01	0.98	0.98	Tm	0.92	0.26	0.33	0.28	0.29
Cr	12.00	14.00	13.00	11.00	4.00	Yb	2.09	1.87	2.03	1.90	2.04
V	10.00	11.00	8.00	8.00	8.00	Lu	0.35	0.31	0.33	0.32	0.32
Rb	227.00	216.00	199.00	212.00	194.00	Y	13.10	10.70	13.30	11.60	12.50
Ba	351.00	350.00	274.00	324.00	252.00	∑REE	74.00	41.67	91.64	77.58	81.00
Sr	128.00	109.00	135.00	129.00	115.00	LREE	63.81	34.29	81.99	69.28	71.90
Ce	29.50	15.80	39.00	33.00	33.90	HREE	9.90	7.38	9.65	8.30	9.10
Pr	3.20	1.60	4.10	3.30	3.61	LREE/HREE	6.45	4.65	8.50	8.35	7.90
Nb	5.70	13.40	14.70	14.60	16.80	$(La/Yb)_N$	5.71	3.43	7.37	6.88	6.48
Ta	1.90	1.50	1.80	1.80	2.10						

4.2.2 Trace elements

The content of ∑REE is (41.67–91.64) × 10^{-6}, and the LREE is (34.29–81.99) × 10^{-6}, the HREE is (7.38–9.90) × 10^{-6}, with LREE/HREE 4.65–8.50, La_N/Yb_N 3.43–7.37, δEu 0.59–0.79, showing the enrichment of the LREE and obvious negative Eu abnormity. The features of the trace elements (Fig. 7, Table 2) suggest that the samples have enrichment of the Rb, Th, U, La, Nd, and deleption of Ba, Sr, Nd, P, Ti.

4.3 Zircon Lu-Hf isotopes

The $^{176}Yb/^{177}Hf$ and $^{176}Lu/^{177}Hf$ of 16 analaysis points of the monzonitic granite are 0.012 712–0.067 712 and 0.000 490–0.002 539 (Table 3), and the $^{176}Lu/^{177}Hf$ is near or less than 0.002, suggesting accumulation of extremely low radiogenic origin ^{176}Hf occurred in the source. Therefore, the $^{176}Hf/^{177}Hf$ can represent the Hf isotope of the source. The $\varepsilon_{Hf}(t)$ values range from -5.54×10^{-3} to 0.99×10^{-3} (Fig. 8), single stage (TDM1) and two stages (TDM2) model ages of Hf isotope are 832–1 082 Ma and 1 068–1 431 Ma (Table 3).

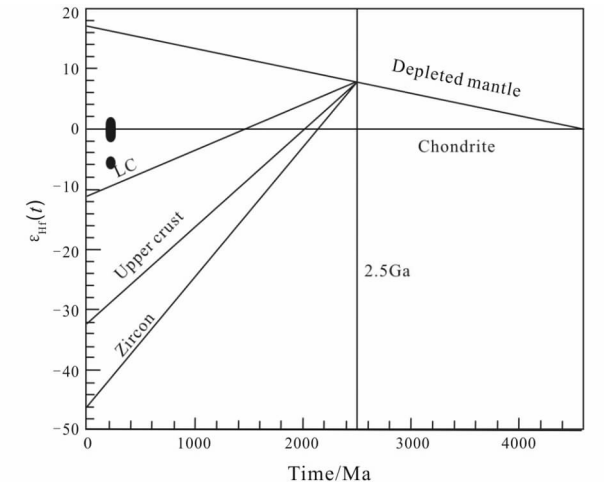

Fig. 8 Zircon Hf isotopic compositions of Hutouya granite

Table 3 LA-ICPMS zircon U-Pb analyses of granite

Testing point	*t*/Ma	$^{176}Hf/^{177}Hf$	1σ	$^{176}Lu/^{177}Hf$	$^{176}Yb/^{177}Hf$	$\varepsilon_{Hf}(0)$	$\varepsilon_{Hf}(t)$	TDM1(Hf)	TDM2(Hf)	fLu/Hf
JR-7-1	221	0.282613	0.000014	0.001245	0.032449	−5.6272456	−0.955350	910.6751	1176.755	−0.96250
JR-7-2	221	0.282645	0.000015	0.002539	0.067712	−4.4751621	0.007976	895.4217	1123.161	−0.92352
JR-7-3	221	0.282629	0.000013	0.001227	0.034499	−5.0513234	−0.376520	887.1644	1144.618	−0.96304
JR-7-4	221	0.282613	0.000014	0.000936	0.023445	−5.6348860	−0.91777	903.5277	1174.696	−0.97181
JR-7-5	221	0.282624	0.000012	0.001252	0.033577	−5.2237901	−0.552700	894.6670	1154.400	−0.96230
JR-7-6	221	0.282645	0.000014	0.000761	0.019365	−4.4999434	0.243238	854.4468	1110.224	−0.97707
JR-7-7	221	0.282631	0.000013	0.001797	0.048016	−4.9704427	−0.378950	897.5665	1144.707	−0.94588
JR-7-8	221	0.282668	0.000015	0.001220	0.033858	−3.6835683	0.992897	832.1718	1068.528	−0.96325
JR-7-9	221	0.282642	0.000011	0.000627	0.016152	−4.6076814	0.155065	855.6891	1115.133	−0.98111
JR-7-10	221	0.282628	0.000013	0.000880	0.022699	−5.0995143	−0.373930	880.9333	1144.502	−0.97350
JR-7-11	221	0.282644	0.000014	0.000900	0.025149	−4.5145954	0.208255	858.1697	1112.158	−0.97288
JR-7-12	221	0.282641	0.000013	0.001207	0.034786	−4.6493582	0.028605	870.5820	1122.117	−0.96365
JR-7-13	221	0.282635	0.000013	0.000490	0.012712	−4.8589253	−0.076190	862.4895	1127.992	−0.98525
JR-7-14	221	0.282665	0.000013	0.002165	0.060837	−3.7800740	0.758144	857.6660	1081.516	−0.93479
JR-7-15	221	0.282654	0.000013	0.000803	0.021612	−4.1616051	0.575655	841.9693	1091.748	−0.97581
JR-7-16	221	0.282481	0.000010	0.000719	0.018511	−10.2892980	−5.542660	1082.0140	1431.053	−0.97836

5 Discussion

5.1 Petrogenesis

The dark minerals in the Hutouya monzonitic granite are mainly Fe-biotite, and the accessory minerals are mainly zircon. The standard mineral calculation of CIPW has minor corundum molecule (<1%) and apatite molecule. The major elements of the sam-

ples have enrichment in Si, K, alkali and depletion of Mg, Ca and Ti, belonging to high-k calc alkaline rock series (Fig. 5a) (Maniar & Piccoli, 1989). The A/CNK is 0.98–1.01, and the A/NK is 1.16–1.20, showing the features of peraluminous granite (Fig. 5b). The patterns of REE show right slope with strong LREE/HREE differentiation and negative Eu abnormity. In the spide map of the trace elements, the rocks are characterized byenrichment of LILE (Rb, Th, U, La, Nd), and deleption of Ba, Sr, Nd, P, Ti.

5.2 Magma source

Zircon is the extremely stable mineral widespread in most of rocks with very high closing temperature of Hf isotopic system, high Hf content and very low Lu / Hf ratio. Therefore, the zircon Hf isotope can be used to trace geological evolution (Wu *et al.*, 2007). The $\varepsilon_{Hf}(t)$ of zircon from monzonitic granite in Hutouya vary from −5.54 to +0.99, coupled with the two-stage model age (TDM2 = 1 068–1 431 Ma), it is suggested that the rocks are derived from the aluminosilicate lower crust with a small amount of new crustal material.

5.3 Tectonic setting

In the Rb/30-Hf-3 * Ta diagram (Fig. 9), the granite samples are mainly located in the post collisional tectonic setting. For the eastern Kunlun, the most intense tectonic-magmatic cycle occurred in Late Paleozoic—Early Mesozoic. During this period, early subduction orogenic stage (260–240 Ma), middle collisional-post collisional orogeny (237–212 Ma) and late intraplate extensional movement occurred (Gao *et al.*, 2012; Mo *et al.*, 2007; Feng *et al.*, 2012; Li *et al.*, 2014). The sedimentology study suggests that the Buqingshan-Animaqing Ocean of the East Kunlun has closed in the middle-Triassic (Wang *et al.*, 1997; Tian *et al.*, 2000; Cai, 2008). In 240 Ma ±, initial collision occurred between the Bayan Harorogenic belt and the East Kunlun block, and the tectonic setting was in the post collisional tectonic evolution stage as late as 225 Ma ± (Cai *et al.*, 2008). During 228–220 Ma, A-type K-riched high differentiation granite suggests that the tectonic setting of the Qimantage has been in the transition from intracontinental orogenic compression to post collisional extension (Feng *et al.*, 2012). The zircon U-Pb age of the Hutouya monzonitic granite is 221 ± 1.7 Ma, belonging to early Late Triassic, when it was the tectonic environment of transformation from compression to extension.

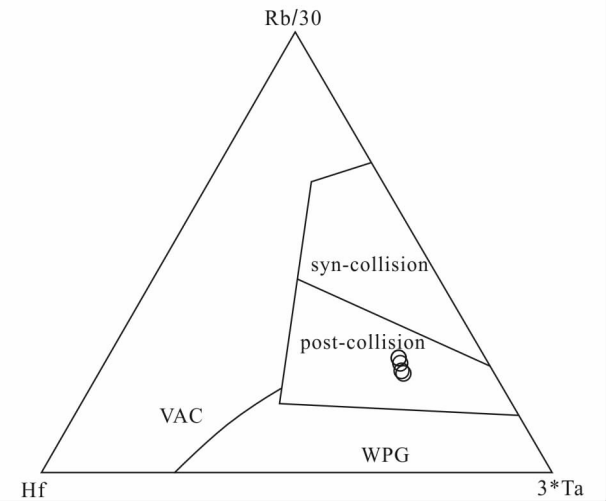

Fig. 9 Diagram of Hf-Rb/30-3Ta for granite

6 Conclusions

(1) The weighted mean zircon LA-ICP-MS U-Pb age of the Hutouya monzonitic granite related to the mineralization is 221 ± 1.7 Ma, belonging to Late Triassic.

(2) Hutouya monzonitic granite is peraluminous and high-k calc alkaline rock series. The rocks have obvious enrichment of LREE and active incompatible element Th and U, and deleption of HFSE (Ba, Sr, Nd, P, Ti), with weak negative Eu abnormity. The homogeneous $\varepsilon_{Hf}(t)$ values range from -5.54×10^{-3} to 0.99×10^{-3} and old two-stage model age TDM2 (1 068–1 431 Ma) suggest that the magma source is mainly aluminosilicate lower crust with a small amount of new crustal material.

(3) The Hutouya monzonitic granite was formed in the tectonic setting of transition from compression to extension of the Bayankala block and the East Kunlun

block.

References

Anderson T. 2002. Correction of common lead in U-Pb analyses that do not report 204Pb. *Chemical Geology*, **192**(1/2): 59-79.

Blichert-Toft J, Chauvel C, Albareúde F. 1997. Separation of Hf and Lu for high-precision isotope analysis of rock samples by magnetic sector-multiple collector ICP-MS. *Contributions to Mineralogy and Petrology*, **127**(3): 248-260.

Cai X F, Luo Z J, Liu D M, *et al*. 2008. One unneglectable stratigraphic unit: Xilikete Group in East Kunlun of Triassic Series. *Journal of Stratigraphy*, **32**(4): 374-380. (in Chinese with English abstract)

Feng C Y, Wang S, Li G C, *et al*. 2012. Middle to Late Triassic granitoids in the Qimantage area, Qinghai Province, China: chronology, geochemistry and metallogenic significances. *Acta Petrologica Sinica*, **28**(2): 665-678. (in Chinese with English abstract)

Feng C Y, Wang X P, Shu X F, *et al*. 2011. Isotopic chronology of the Hutouya skarn lead zinc polymetallic ore district in Qimantage area of Qinghai Province and its geological significance. *Journal of Jilin University: Earth Science Edition*, **41**(6): 1806-1817. (in Chinese with English abstract)

Fisher C M, Vervoot J D, Hanchar J M. 2014. Guidelines for reporting zircon Hf isotopic data by LA-MC-ICPM Sand potential pitfalls in the interpretation of these data. *Chemical Geology*, **363**: 125-133.

Gao Y B, Li W Y, Ma X G, *et al*. 2012. Genesis geochronology and Hf isotopic compositions of the magmatic rock in Galinge iron deposit, eastern Kunlun. *Journal of Lanzhou University: Natural Sciences*, **48**(2): 36-47. (in Chinese with English abstract)

Hu Z C, Liu Y S, Gao S, *et al*. 2012. Improved in situ Hf isotope ratio analysis of zircon using newly designed X skimmer cone and jet sample cone in combination with the addition of nitrogen by laser ablation multiple collector ICP-MS. *Journal of Analytical Atomic Spectrometry*, **27**(9): 1391-1399.

Li X, Yuan W M, Hao N N, *et al*. 2014. Characteristics and tectonic setting of granite in Wulonggou area, East Kunlun Mountains. *Global Geology*, **33**(2): 275-288. (in Chinese with English abstract)

Liu Y S, Gao S, Hu Z C, *et al*. 2010. Continental and oceanic crust recycling-induced melt-peridotite interactions in the trans-north China orogen: U-Pb dating, Hf isotopes and trace elements in zircons from mantle xenoliths. *Journal of Petrology*, **51**(1/2): 537-571. (in Chinese with English abstract)

Liu Y S, Hu Z C, Gao S, *et al*. 2008. In situ analysis ofmajor and trace elements anhydrous minerals by LA-ICP-MS without applying an internal standard. *Chemical Geology*, **257**(1/2): 34-43. (in Chinese with English abstract)

Ludwig K R. 2003. User's manual for isoplot 3.00: a geochronological toolkit for Microsoft Excel. [s. l.]: Berkeley Geochronology Center Special Publication, 70.

Maniar P D, Piccoli P M. 1989. Tectonic discrimination of granitoids. Geological Society of America Bulletin, **101**(4):635-643.

Mo X X, Luo Z H, Deng J F, *et al*. 2007. The granite and crust growth in East Kunlun orogenicbelt. *Geological Journal of China Universities*, **13**(3): 403-414. (in Chinese with English abstract)

Qi L, Hu J D, Gregoire D C. 2000. Determination of trace elements in granites by inductively coupled plasma mass spectrometry. *Talanta*, **51**: 507-513.

Tian J, Zhang K X, Gong Y M. 2000. The research progress of Middle Triassic series in eastern Kunlun. *Earth Science*, **25**(3): 290-294. (in Chinese with English abstract)

Wang Y B, Huang J C, Luo M S, *et al*. 1997. The evolutionary history of the oceanic basins in southern of East Kunlun orogen during Hercynian--Early Indosinian period. *Earth Science*, **22**(4): 369-372.

Wu F Y, Li X H, Zheng Y F, *et al*. 2007. Lu-Hf isotopic systematics and their applications in petrology. *Acta Petrologica Sinica*, **23**(2): 185-220. (in Chinese with English abstract)

Yuan H L, Gao S, Liu X M, *et al*. 2004. Accurate U-Pbage and trace element determinations of zircon by laserablation-inductively coupled plasma-mass spectrometry. *Geostandards and Geoanalytical Research*, **28**(3): 353-370.

Yuan H L, Wu F Y, Gao S, *et al*. 2003. Determination of U-Pb age and rare earth element concentrations of zircons from Cenozoic intrusion in northeastern China by laser ablation ICP-MS. *Chinese Science Bulletin*, **48**(14): 1511-1520. (in Chinese with English abstract)

Zhang A K, Liu G L, Feng C Y, *et al*. 2013. Geochemical characteristics and ore-controlling factors of Hutouya polymetallic deposit , Qinghai Province. *Mineral Deposits*, **21**(1): 94-108. (in Chinese with English abstract)

Zhang X F. 2012. Genesis discussion on the Hutouya polymetallic deposit in Qimantage area, East Kunlun, Qinghai, China: doctor degree's thesis. Xi'an: Chang'an University. (in Chinese with English abstract)